Supplementary Information for

Tracking lysosomal polarity variation in inflamed, obese, and cancer mice guided by a fluorescence sensing strategy

Junling Yin, Min Peng, and Weiying Lin*

Institute of Fluorescent Probes for Biological Imaging, School of Materials Science and Engineering, School of Chemistry and Chemical Engineering, University of Jinan, Shandong 250022, P.R. China.
E-mail: weiyinglin2013@163.com

Table of Contents

Materials and instruments

Unless otherwise stated, all reagents were purchased from commercial suppliers and used without further purification. Fluorescence spectra were measured on a HITACHI F4600 fluorescence spectrophotometer. MTT was purchased from J&K Scientific Ltd. UV-vis absorption spectra were obtained on a Shimadzu UV-2700 spectrophotometer. The pH measurements were performed with a Mettler-Toledo Delta 320 pH meter. TLC analysis carried out on silica gel plates and column chromatography was conducted over silica gel (mesh 200-300), both of them were purchased from the Qingdao Ocean Chemicals. ^{1}H and ^{13}C NMR spectra were measured on an AVANCE III digital NMR spectrometer, using tetramethylsilane (TMS) as internal reference. High resolution mass spectrometric (HRMS) analyses were measured on an Agilent 1100 HPLC/MSD spectrometer. Melting point was measured with X-5 micro melting point tester. Cell imaging experiment was performed on Nikon A1 Fluorescence Microscopy equipped with a cooled CCD camera. PerkinElmer IVIS spectrum imaging system equipped with COM 8 X-ray controller and -90 °C CCD camera. The animals were purchased from School of Pharmaceutical Sciences, Shandong University, and the studies were approved by the Animal Ethical Experimentation Committee of Shandong University. All animals were kindly kept during experiment according to the requirements of the National Act on the use of experimental animals (China).

Synthesis routine of MND-Lys

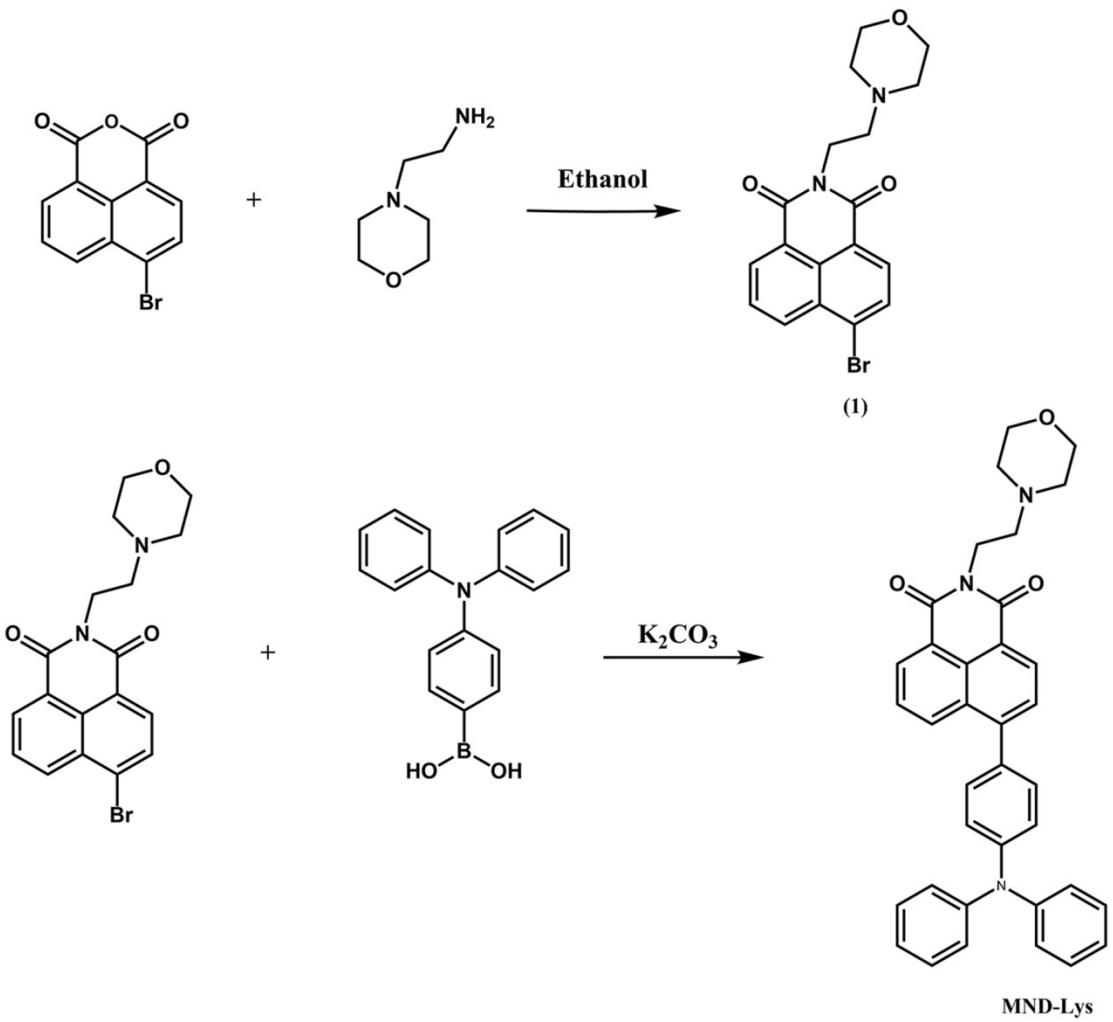

Scheme S1. The synthetic routine of **MND-Lys**.

Synthesis of compound 1

4-Bromo-1,8-naphthalic anhydride 277 mg (1 mmol) and 4-(2-Aminoethyl)-morpholine 169 mg (1.3 mmol) were added to 2 mL of ethanol, and the reaction mixture was heated to reflux for 2 h. After cooled to room temperature, the mixture was filtered and dried to afford the desired product as a gray solid 315 mg with a yield of 85 %. ^{1}H NMR (400 MHz, CH_2Cl_2-d_2) δ 8.58 (dd, J1 = 7.4, J2 = 2.0 Hz, 1H), 8.52 (dd, J1= 8.4, J2 = 1.2 Hz, 1H), 8.34 (d, J = 8.0 Hz, 1H), 8.02 (d, J = 8.0 Hz, 1H), 7.82 (dd, J1 = 8.4, J2 = 7.2 Hz, 1H), 4.27 (t, J = 6.8 Hz, 2H), 3.61 (t, J = 4.6 Hz, 4H), 2.65 (t, J = 6.8 Hz, 2H), 2.54 (t, J = 4.6 Hz, 4H). ^{13}C NMR (101 MHz, DMSO-d6) δ 162.84,

162.79, 132.62, 131.60, 131.35, 130.98, 129.77, 129.15, 128.79, 128.24, 122.66, 121.88, 66.18, 55.43, 53.37, 36.90. HRMS (ESI): calcd. For $C_{18}H_{17}BrN_2O_3$, $[M+H]^+$, m/z, 388.2490, found: 388.3422. The melting point of compound **1** was about 75.4 °C.

Compound **1** (2mmol; 278 mg), 4-(diphenylamino)phenylboronic acid (2 mmol; 578 mg), Tetrakis(triphenylphosphine)palladium (0.05 mmol; 57 mg) and K_2CO_3 (6 mmol; 828 mg) were added into tetrahydrofuran (THF). Then the mixture was protected by nitrogen and refluxed at 60 °C for 12 h. The progress of the reaction was monitored by TLC. The crude products were further purified by silica gel column (ethyl acetate/petroleum ether =1:5) to afford 75%. ^{1}H NMR (400 MHz, Chloroform-d) δ 8.67 (m, 2H), 8.46 (dd, J_1 = 8.6, J_1 = 1.0, Hz, 1H), 7.77 (t, J = 8.2 Hz, 2H), 7.38 (m, 6H), 7.25 (J = 4.4 Hz, 6H), 7.14 (t, J = 7.4 Hz, 2H), 4.42 (t, J = 7.0 Hz, 2H), 3.74 (J = 4.4 Hz,, 4H), 2.78 (t, J = 6.8 Hz, 2H), 2.67 (s, 4H); ^{13}C NMR (101 MHz, $CDCl_2$-d2) δ 164.29, 148.64, 147.74, 146.99, 134.94, 133.02, 132.41, 131.19, 131.14, 130.96, 130.36, 129.74, 129.47, 129.30, 127.94, 126.96, 125.27, 124.73, 124.42, 123.87, 123.27, 123.13, 122.96, 122.88, 67.28, 67.10, 56.41, 54.22, 53.55, 37.58. HRMS (ESI): calcd. For $C_{36}H_{31}N_3O_3$, $[M+H]^+$, m/z, 554.2399, found: 554.2435. The melting point of the probe **MND-Lys** was around 91.6 °C.

Calculation of fluorescence quantum yield of MND-Lys

The fluorescence quantum yields (Φ_f) were determined using fluorescein as the reference according to the literature method. Quantum yields were corrected as follows:

$$\emptyset_f = \emptyset_r\left(\frac{A_r{\eta_s}^2 D_s}{A_s{\eta_s}^2 D_r}\right)$$

Where the s and r represent designate the sample and reference samples, respectively. A is the absorbance at λ_{ex}, η is the average refractive index of the appropriate solution, and D is the integrated area under the corrected emission spectrum.

Calculation of two-photon absorption cross section of MND-Lys.

$$\delta = \delta_{ref} \frac{F \Phi_{ref} C_{ref} n_{ref}}{F_{ref} \Phi C n}$$

where "ref" subscript stands for reference while the ones without any are for the sample. δ: Two photon absorption cross section; F: Integrated area of two photon Induced fluorescence spectra; Φ: Fluorescence quantum yield; C: Concentration in moles/Litre, n: Refractive Index of the solvents used.

Optical property test of the MND-Lys

The stock solution of **MND-Lys** (1 mM) was dissolved in DMSO. 10 μM of the probe was used in spectral test by addition of 30 μL stock solution to 3.0 mL different polarity solutions include cyclohexane, toluene, dioxane, tetrahydrofuran (THF), Ethyl acetate (EA), Chloroform, dichloromethane (DCM), acetone. Different viscosity test systems were carried out in mixture of glycerol and methanol with various volume ratios. The resulting solution was shaken well before recording the spectra. For all the measurements, the excitation wavelength, excitation slit widths, and emission slit widths are 450 nm, 5 nm, and 5 nm, respectively.

Cell culture and cell cytotoxicity assays

Cell culture

4T1 cell were utilized in this work. These cells were cultured in Dulbecco's Modified Eagle Medium media (DMEM, Hyclone) supplemented with 10% heat-inactivated fetal bovine serum (FBS, Sijiqing) and 1% antibiotics (100 U/mL penicillin and 100 μg/mL streptomycin, Hyclone) at 37 °C and 5% CO_2.

Cytotoxicity assays

The cytotoxicity of the probe **MND-Lys** to 4T1 cells were studied by standard MTT assays. 2×10^4 cells/mL cells were seeded in 96-well plates and then incubated with various concentrations of **MND-Lys** (0-50 μM) for 24 h. After that, 10 μL of

MTT (5 mg/mL) was added to each well and incubated for another 4 h. Finally, the media was discharged, and 100 μL of DMSO was added to dissolve the formazan crystals. The plate was shaken for about 10 min, and each well was analyzed by the microplate reader and detected at the absorbance of 490 nm. The cell viability (%) = (OD_{sample} - OD_{blank}) / ($OD_{control}$ - OD_{blank}) × 100%. OD_{sample}, $OD_{control}$, and OD_{blank} denote the cells incubated with various of concentrations of the probe, the cells without the probe, and the wells containing only the culture media, respectively.

Cell imaging and colocalization experiment

Before imaging, 1 mL of cells was seeded in the glass bottom culture dishes (Nest) with the density of 1×10^5/mL. The cells were placed on glass cover slips and allowed to adhere for 24 h. When the cells reached about 70% confluence, they were processed separately according to the experimental requirements for imaging experiments. One group of cells were cultured in PBS for 6 h, and **MND-Lys** (10 μM) for another 30 min. Another group of cells were incubated with sucrose (2.0 mM, 20 min) and **MND-Lys** (10 μM) for 30 min. Finally, confocal fluorescence imaging was carried out using Nikon fluorescence microscope equipped with the excitations of 488 nm (one-photon mode) and 800 nm (Two-photon mode), and the collection is 500-550 nm.

The co-localization experiments were carried out with commercially available dye Lysosomal Red and Nile Red, respectively. Firstly, one group of cells were incubated with Lysosomal Red (5.0 μM) and probe **MND-Lys** (10.0 μM) simultaneously for 30 min; another group of cells were incubated with Nile Red (2.0 μM) and **MND-Lys** (10.0 μM) simultaneously for 30 min. Then, cells were imaged after washed by PBS for three times. The green channel was collected at 500-550 nm with the excitation of 488 nm. The red channel at 570-620 nm was collected with the excitation of 561 nm.

In situ cell spectroscopy acquisition experiments

In situ cell spectroscopy acquisition was obtained by the lambda stacking function of the confocal microscope. Before acquisition spectrum, confocal fluorescence imaging was firstly carried out in the channel mode of confocal microscopy to find proper cells. The imaging condition was set to 488 nm excitation and 500-500 nm collection. After cell imaging, the imaging mode was switched to the spectral acquisition mode, at which the position of the cell imaging disk remains unchanged to ensure that cells in imaging mode and spectral acquisition are identical. Then the in-situ emission spectra were obtained by the lambda stacking function of the confocal microscope. With such function, the precise in-situ emission spectra could be obtained, and the emission peaks could be clearly observed.

Preparation of living organs and tumor for imaging experiments

Four-week old female balb/c mice were purchased from School of Pharmaceutical Sciences, Shandong University, and the studies were approved by the Animal Ethical Experimentation Committee of Shandong University. All animals were kindly kept during experiment according to the requirements of the National Act on the use of experimental animals (China).

The mice were inoculated with 4T1 cell and after 12 days a tumor was obtained. Then the organs (heart, liver, spleen, lung and kidney) and tumor were isolated from the mice. After washing by PBS (pH 7.4) for three times, these isolated organs and tumor were loaded with **MND-Lys** (20 μM), respectively, and finally subjected to imaging using an IVIS Lumina XR *in vivo* imaging system with an excitation filter of 500 nm and an emission filter of 560 nm.

Preparation of mice tumor slices for imaging experiments

The slices were prepared from the tumor of 12-day inoculated mice, and they were cut to 200 mm thickness by using a vibrating-blade microtome in 25 mM PBS (pH

7.4). The slices were incubated with 15 μM **MND-Lys** in PBS buffer bubbled with 95% O_2 and 5% CO_2 for 0.5 h at 37 °C, and then washed three times with PBS, transferred to the glass bottomed dishes, and observed under two-photon confocal microscope (Nikon AMP1). The fluorescence images of the slices were acquired using 800 excitation and fluorescence emission windows of 500-550 nm.

Fluorescence imaging of polarity in different period zebrafish

Wild type zebrafish were obtained from the Nanjing Eze-Rinka Biotechnology Co., Ltd. For the fluorescence imaging experiments, adult zebrafishe and zebrafish embryos were transferred into a 30 mm glass culture dishes using a disposable sterilized dropper. 10 μM probe **MND-Lys** was added for 30 min, followed by washing away gently. After that, the zebrafish were transferred into the new glass bottom dishes for imaging. Prior to the imaging, we adopted 1% agarose gel for immobilization of zebrafish, and put zebrafish onto agarose with a little media to ready imaging. Fluorescence images were acquired using Nikon A1R confocal microscope with a 4 × objective lens. The imaging experiments were recorded through a Nikon AIP confocal microscopy. The fluorescence emission was collected at TRICT channel (500-550 nm) upon 488 nm excitation at one-photon mode and 800 nm at two-photon mode.

Construction of an inflammatory mice model for imaging experiment

The animals were purchased from School of Pharmaceutical Sciences, Shandong University, and the studies were approved by the Animal Ethical Experimentation Committee of Shandong University. All animals were kindly kept during experiment according to the requirements of the National Act on the use of experimental animals (China).

Four-week old female balb/c mice were purchased from School of Pharmaceutical Sciences, Shandong University and the mice were kindly kept during the experiments. These mice were injected by LPS in abdomen respectively to produce inflammation

models. After two days, the triggered mice and normal mice were simultaneously utilized for *in vivo* imaging. Before *in vivo* imaging, the abdominal fur was removed by an electric shaver, and then the mice were anesthetized by 4% chloral hydrate aqueous solution (100 μL). The probe **MND-Lys** (80 μL; 1 mM) was then injected into the abdominal position of the normal mice and triggered mice, respectively. The mice were then imaged by using an *in vivo* imaging system with an excitation filter of 500 nm and an emission filter of 560 nm.

Construction of obesity mice model for imaging experiment

The animals were purchased from School of Pharmaceutical Sciences, Shandong University, and the studies were approved by the Animal Ethical Experimentation Committee of Shandong University. All animals were kindly kept during experiment according to the requirements of the National Act on the use of experimental animals (China).

Mice were fed high-fat forage for inducing obesity mice model. We tracked the weight of the mice in, and the model group was considered successful when the weight of the mice was greater than 120% of the control group. After that, the obese mice and normal mice were simultaneously utilized for *in vivo* imaging. Before *in vivo* imaging, the abdominal fur was removed by an electric shaver, and then the mice were anesthetized by 4% chloral hydrate aqueous solution (100 μL). The probe **MND-Lys** (80 μL; 1 mM) was then injected into the abdominal position of the normal mice and triggered mice, respectively. The mice were then imaged by using an *in vivo* imaging system with an excitation filter of 500 nm and an emission filter of 560 nm.

Construction of tumor-bearing mice model for imaging experiment

The animals were purchased from School of Pharmaceutical Sciences, Shandong University, and the studies were approved by the Animal Ethical Experimentation Committee of Shandong University. All animals were kindly kept during experiment according to the requirements of the National Act on the use of experimental animals

(China).

4T1 cells were grafted into the mice to produce tumor models and on day 12 post-injection, a tumor was obtained. Then the tumor-bearing mice and normal mice were simultaneously utilized for *in vivo* imaging. Before *in vivo* imaging, the abdominal fur was removed by an electric shaver. Then the mice were anesthetized by 4% chloral hydrate aqueous solution (100 μL). **MND-Lys** (80 μL; 1 mM) was then injected into the abdominal position of the normal mice and tumor-grafted mice by hypodermic injection, respectively. The mice were then imaged by using an i*n vivo* imaging system with an excitation filter of 500 nm and an emission filter of 560 nm.

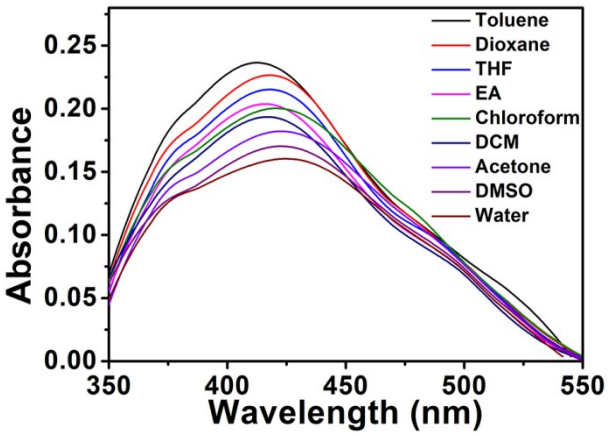

Fig. S1 The absorption spectra of **MND-Lys** in different polarity solvents. Concentration = 10 μM. Water：pH 7, 37 °C, and about 100 mM ionic strength.

Table S1. The photophysical properties of **MND-Lys** in the different solvents. $E_T(30)$ is the empirical parameter for solvent polarity. Φ_f is the fluorescence quantum yield of **MND-Lys** in various polarity solvents.

Solvents	$E_T(30)$	λ_{abs}/nm	λ_{em}/nm	Stokes shift/ nm	Φ_f/%
Toluene	33.9	411	537	126	30.8
Dioxane	36.0	412	559	147	25.6
THF	37.4	415	584	174	17.2
Ethyl acetate	38.1	417	592	175	15.2
Chloroform	39.1	418	598	180	14.6
DCM	40.7	417	609	192	13.4
Acetone	42.2	420	624	204	2.3
DMSO	45.1	422	643	221	0.9

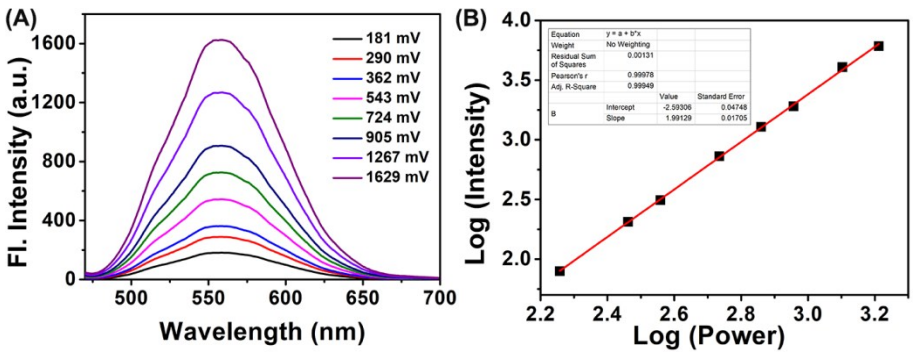

Fig. S2 (A) Laser power-dependent two-photon emission spectra of **MND-Lys (**10 μm**)** in dioxane. (B) The logarithmic plots between the power dependence and relative two-photon induced luminescence intensity.

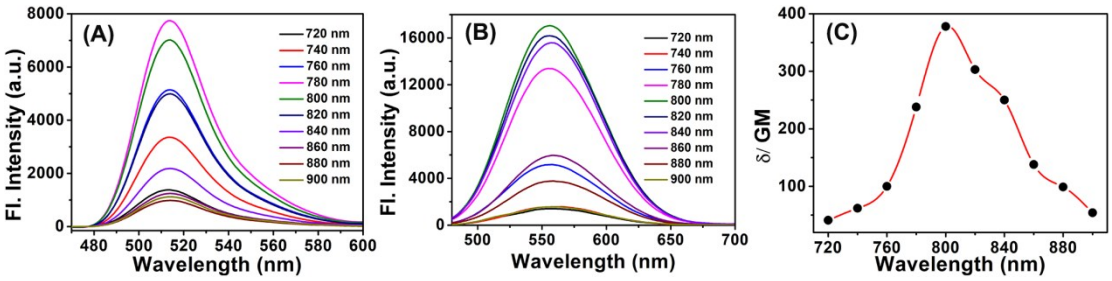

Fig. S3 Two-photon fluorescence intensity of (A) 1.0 μM fluorescein and (B) 10.0 μM **MND-Lys** at 720-900 nm excitations. (C) two-photon absorption cross sections (δ) of the compound **MND-Lys** at 720-900 nm in dioxane.

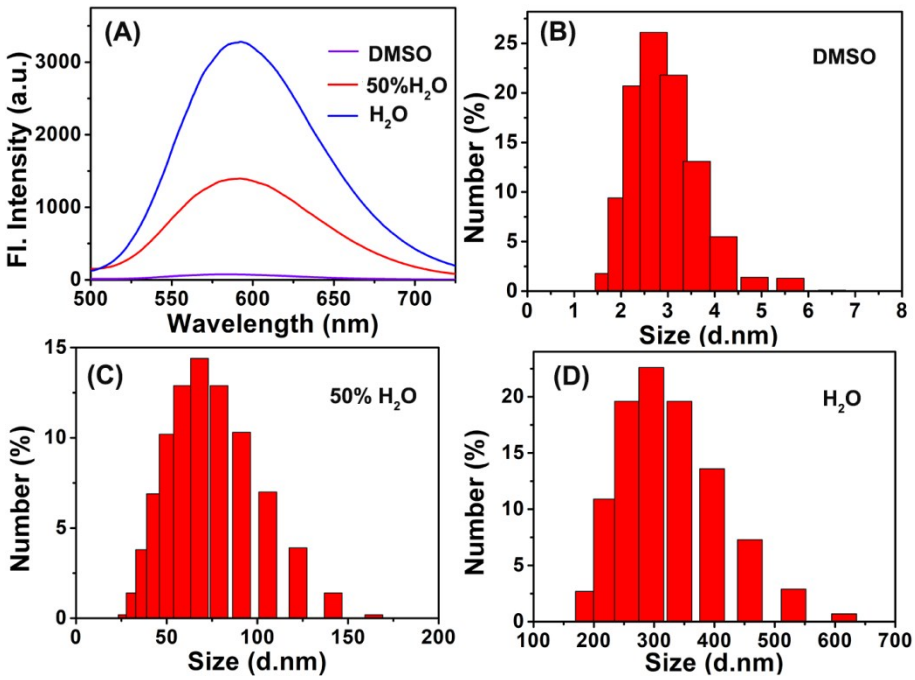

Fig. S4 (A) Fluorescence spectra of 10 μM **MND-Lys**. DLS measurements of **MND-Lys** in DMSO (B), 50% H_2O (C) and H_2O solutions (D). DMSO: spectrally pure; H_2O: pH 7, 37 °C, and 100 mM ionic strength.

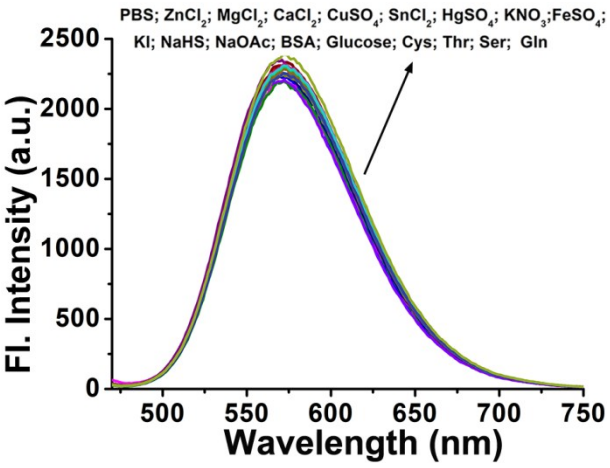

Fig. S5 The relative fluorescence intensities of **MND-Lys** (10 μM) to various relevant analytes in phosphate buffer (pH 7.4, 10 μM, 5% DMSO). 1. Only ; 2, $ZnCl_2$ (1.0 mM); 3, $MgCl_2$ (1.0 mM); 4, $CaCl_2$ (1.0 mM); 5, $CuSO_4$ (1.0 mM); 6, $SnCl_2$ (1.0 mM); 7, $HgSO_4$ (1.0 mM); 8, KNO_3 (1.0 mM); 9, $FeSO_4$ (1.0 mM); 10, KI (1.0 mM); 11, NaHS (1.0 mM); 12, NaOAc (1.0 mM); 13, BSA (10%); 14, glucose (1.0 mM) ; 15, Cys (500 μM); 16, Thr (500 μM); 17, Ser (500 μM); 18, Gln (500 μM).

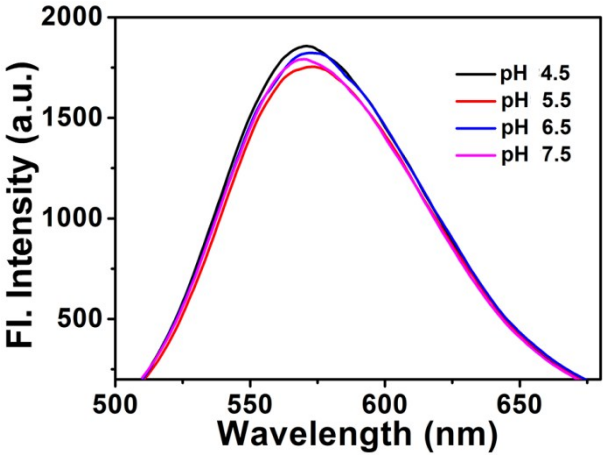

Fig. S6 The fluorescence spectra of **MND-Lys** in different pH values.

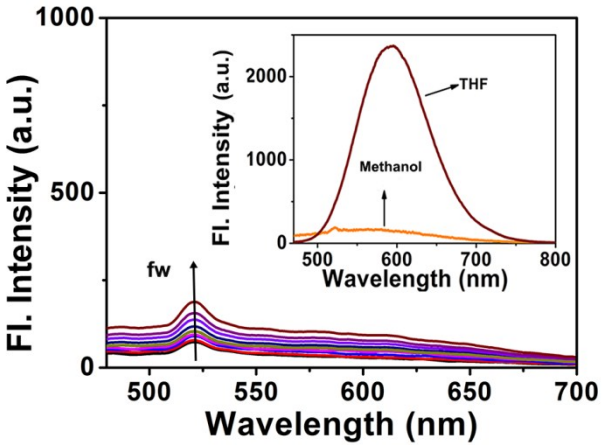

Fig. S7 The fluorescence spectra of **MND-Lys** (10 μM) under different viscosity in methanol-glycerol system with the fraction of glycerol (f_w) from 0 to 100%. The inside figure is that the fluorescence spectra of **MND-Lys** in THF and methanol. THF and methanol have almost the same viscosity (0.53 cP vs 0.60 cP) but different polarity ($E_T(30)$ = 37.4 *vs* 55.4).

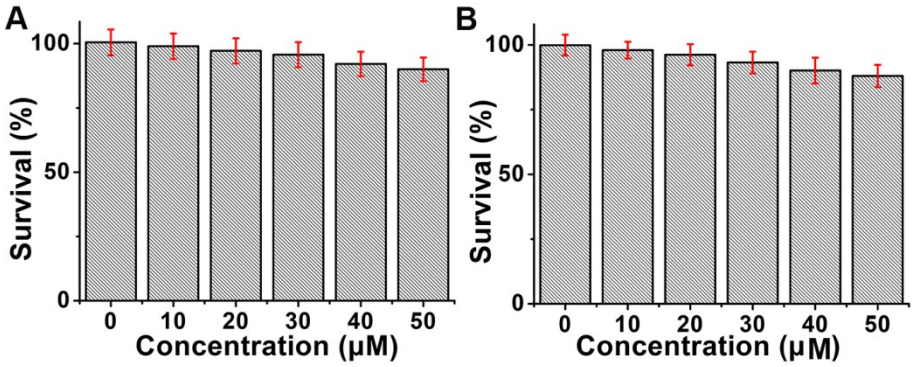

Fig. S8 The MTT experiments of **MND-Lys** with different concentrations for Hela cells (A), 4T1 cells (B).

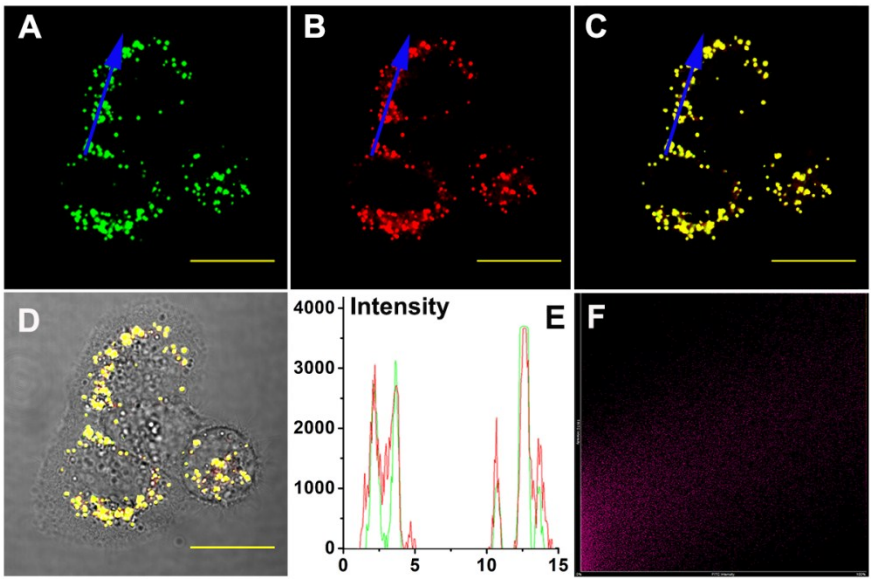

Fig. S9 Images of the living Hela cells costained with (A) 10.0 μM **MND-Lys** (λ_{ex} = 488 nm, λ_{em} = 500-550 nm), (B) 5.0 μM Lysosomal Red (λ_{ex} = 561 nm, λ_{em} = 570-620 nm). (C) The merged pattern of (A) and (B). (D) Merge field (E) Intensity profile of ROI across the cells in the green and red channels. (F) The intensity scatter plot of two channels. Scale bar: 20 μm.

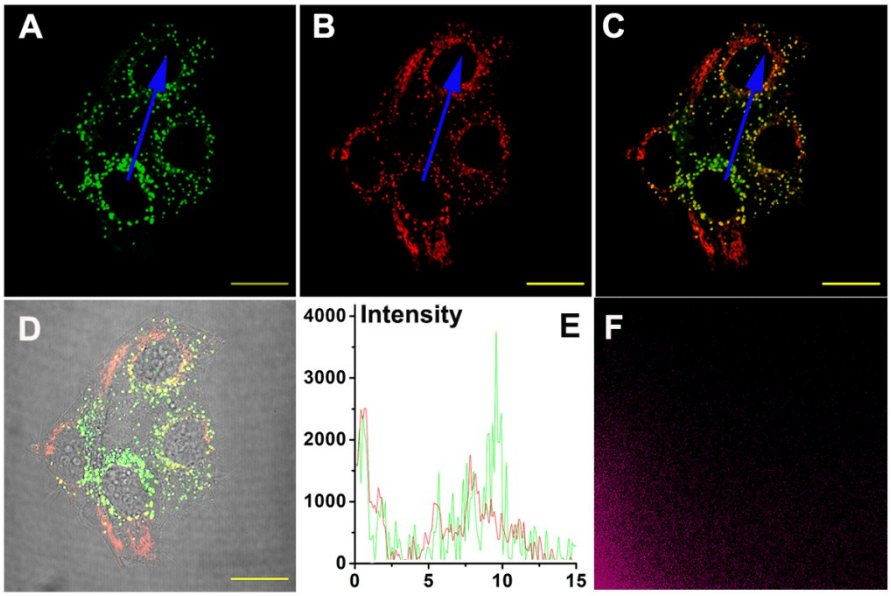

Fig. S10 Images of the living Hela cells costained with (A) 10.0 μM **MND-Lys** (λ_{ex} = 488 nm, λ_{em} = 500-550 nm), (B) 2.0 μM Nile Red (λ_{ex} = 561 nm, λ_{em} = 570-620 nm). (C) The merged pattern of (A) and (B). (D) Merge field (E) Intensity profile of ROI across the cells in the green and red channels. (F) The intensity scatter plot of two channels. Scale bar: 20 μm.

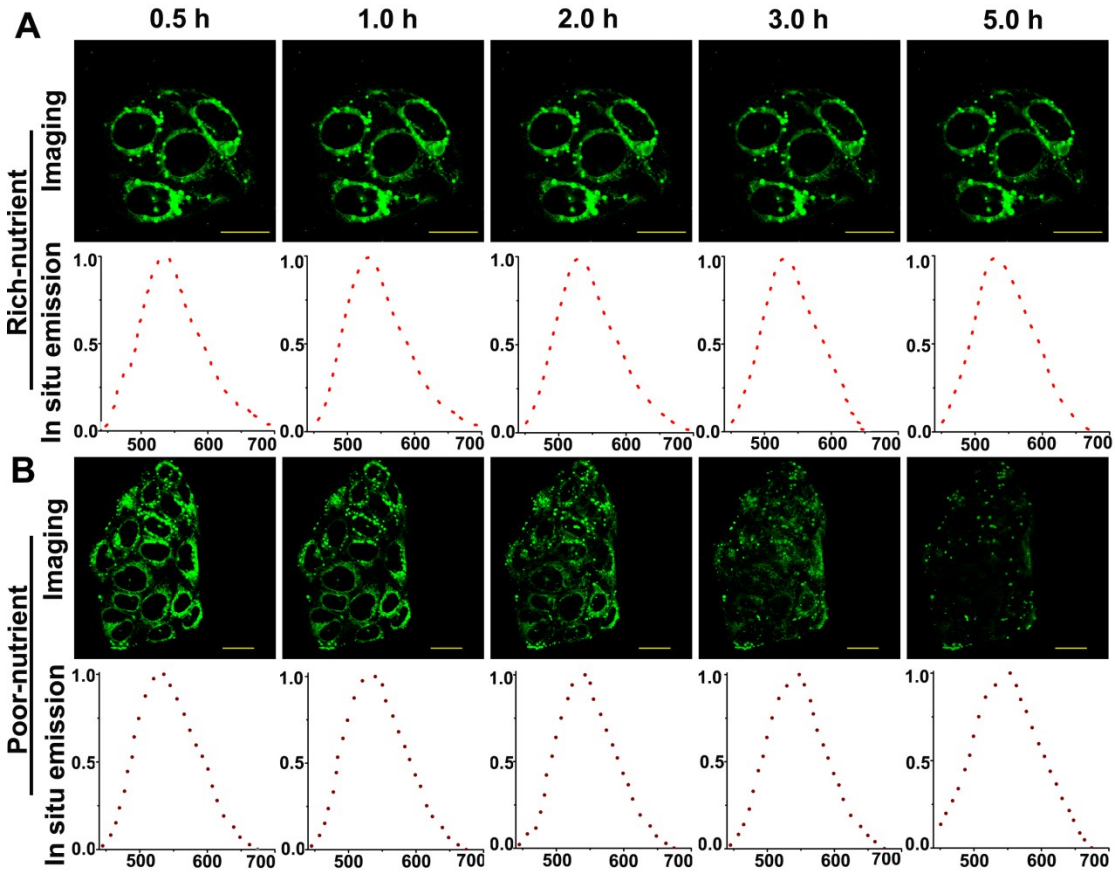

Fig. S11 (A) Real-time confocal imaging and in site emission of Hela cells at rich-nutrient conditions. (B) Real-time confocal imaging and in site emission of Hela cells at poor nutrient conditions. λ_{ex} = 488 nm, λ_{em} = 500-550 nm.

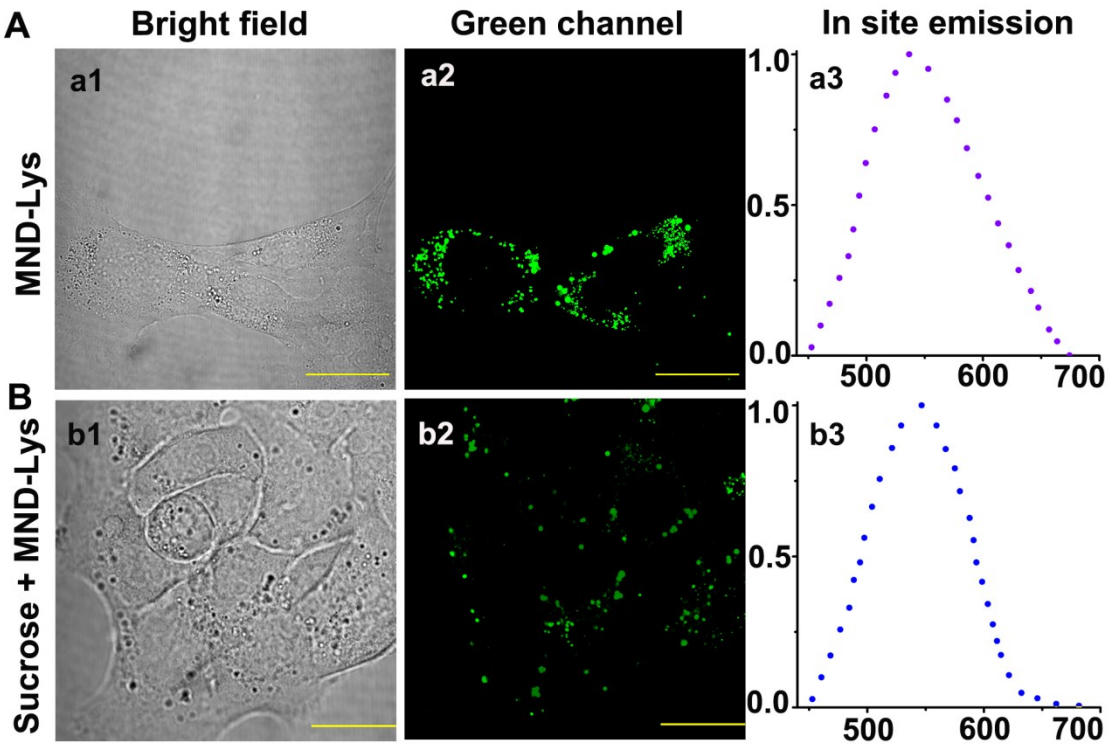

Fig. S12 (A) Fluorescence imaging of Hela cells incubate with 10 μM **MND-Lys**: (a1) Bright field; (a2) Green channel. (a3) In site emission spectrum. (B) Fluorescence imaging of Hela cells incubate with sucrose (2.0 mM) + **MND-Lys** (10 μM): (b1) Bright field; (b2) Green channel; (b3) In site emission spectrum. The images were collected at 500-550 nm; scale bar: 20 μm.

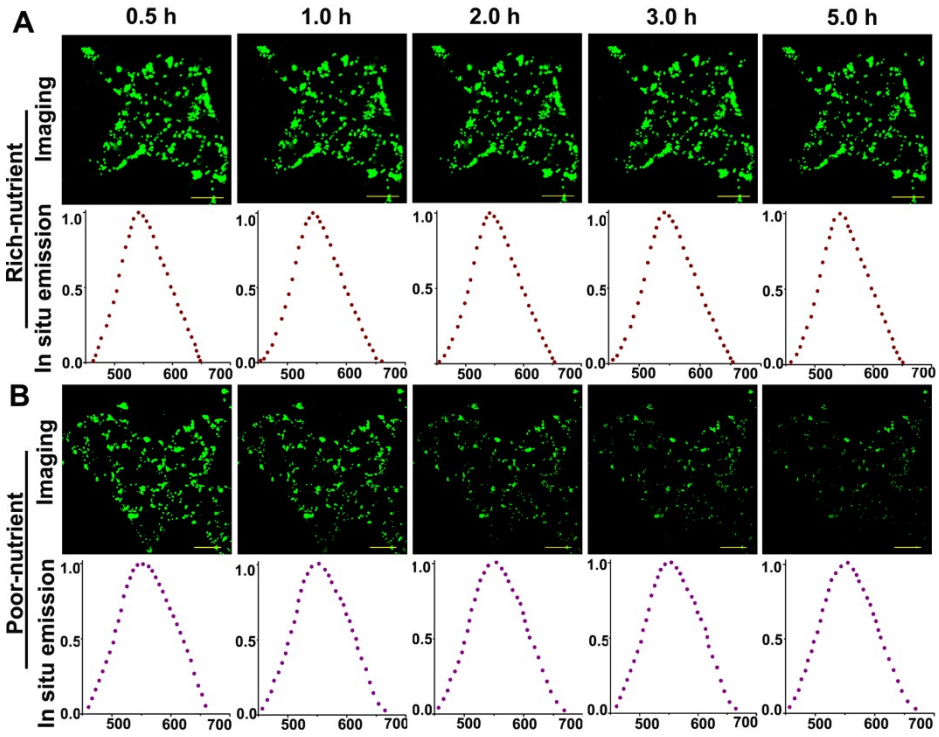

Fig. S13 (A) Real-time confocal imaging and in site emission of SiHa cells at rich-nutrient conditions. (B) Real-time confocal imaging and in site emission of SiHa cells at poor nutrient conditions. λ_{ex} = 488 nm, λ_{em} = 500-550 nm.

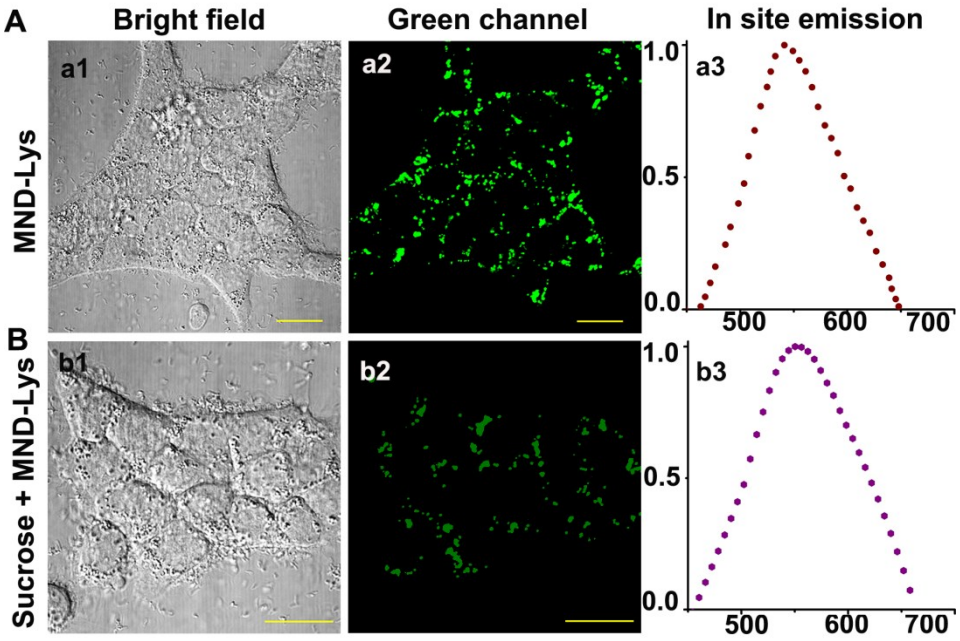

Fig. S14 (A) Fluorescence imaging of SiHa cells incubate with 10 μM **MND-Lys**: (a1) Bright field; (a2) Green channel. (a3) In site emission spectrum. (B) Fluorescence imaging of SiHa cells incubate with sucrose (2.0 mM) + **MND-Lys** (10 μM): (b1) Bright field; (b2) Green channel; (b3) In site emission spectrum. The images were collected at 500-550 nm; scale bar: 20 μm.

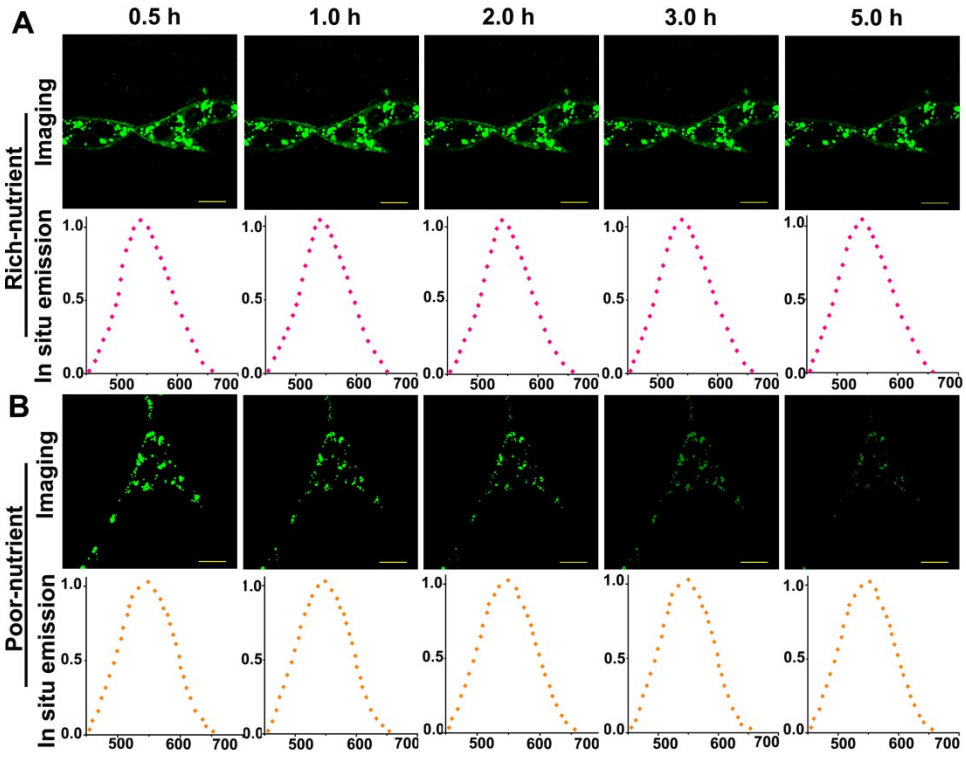

Fig. S15 (A) Real-time confocal imaging and in site emission of Fibroblast cells at rich-nutrient conditions. (B) Real-time confocal imaging and in site emission of Fibroblast cells at poor nutrient conditions. λ_{ex} = 488 nm, λ_{em} = 500-550 nm.

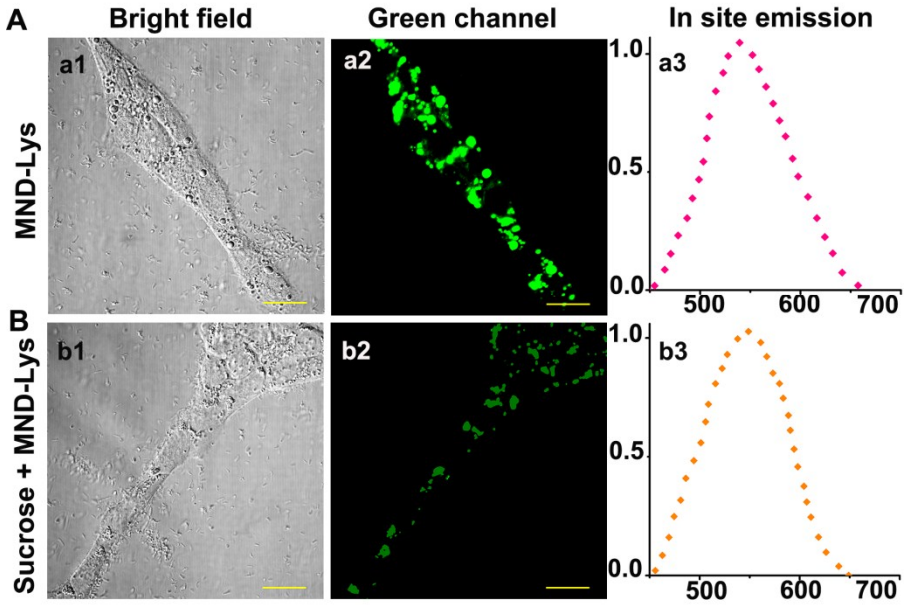

Fig. S16 (A) Fluorescence imaging of Fibroblast cells incubate with 10 μM **MND-Lys**: (a1)Bright field; (a2) Green channel. (a3) In site emission spectrum. (B) Fluorescence imaging of Fibroblast cells incubate with sucrose (2.0 mM) + **MND-Lys** (10 μM): (b1) Bright field; (b2) Green channel; (b3) In site emission spectrum. The images were collected at 500-550 nm; scale bar: 20 μm.

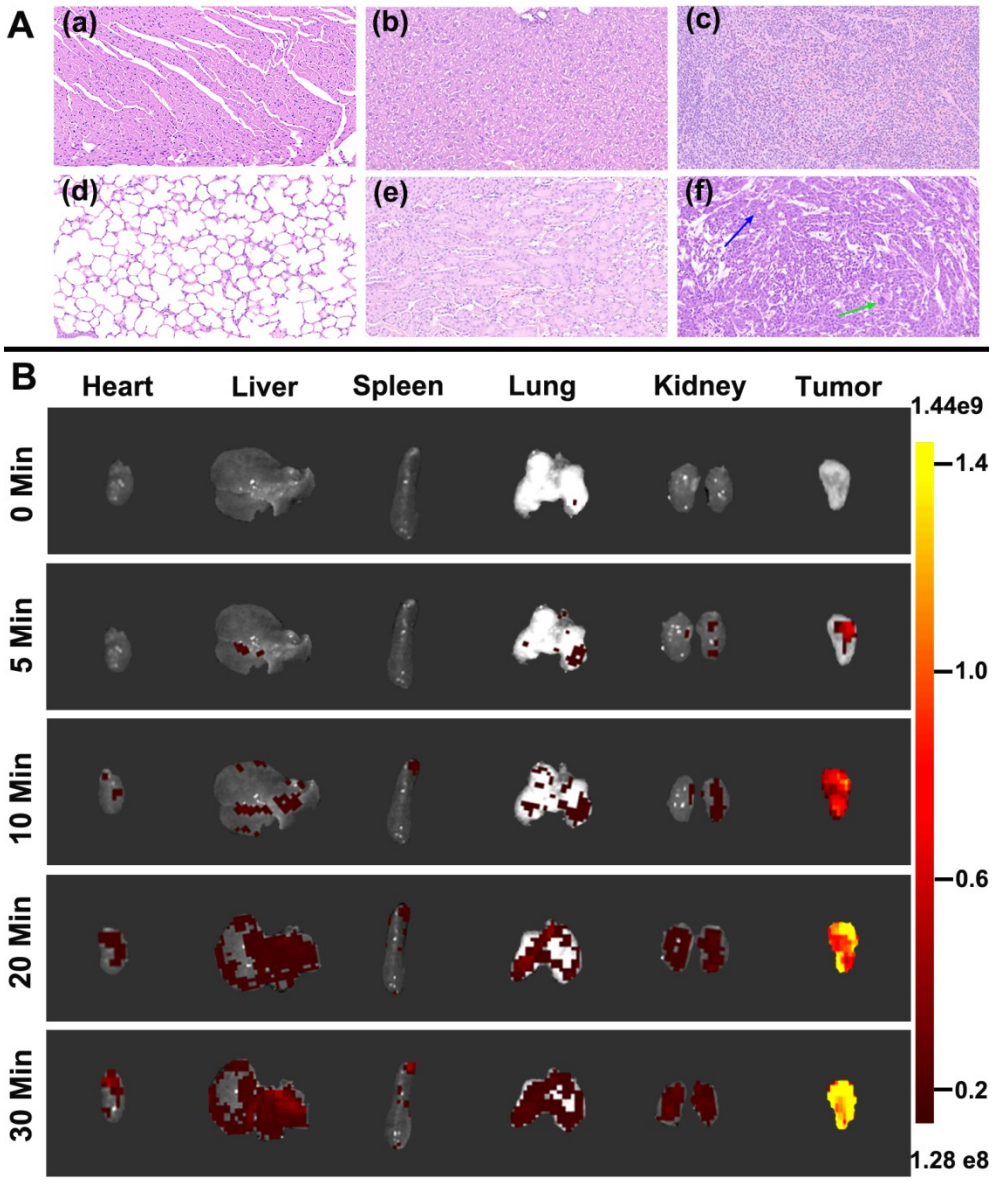

Fig. S17 (A) HE staining of heart (a), liver (b), spleen (c), lung (d) and tumor (f). (B) Time-dependent fluorescence imaging of lysosome polarity with **MNDLys** in living organs and tumor. Concentration: 15 μM; λ_{ex} = 500 nm, λ_{em}=560 nm.

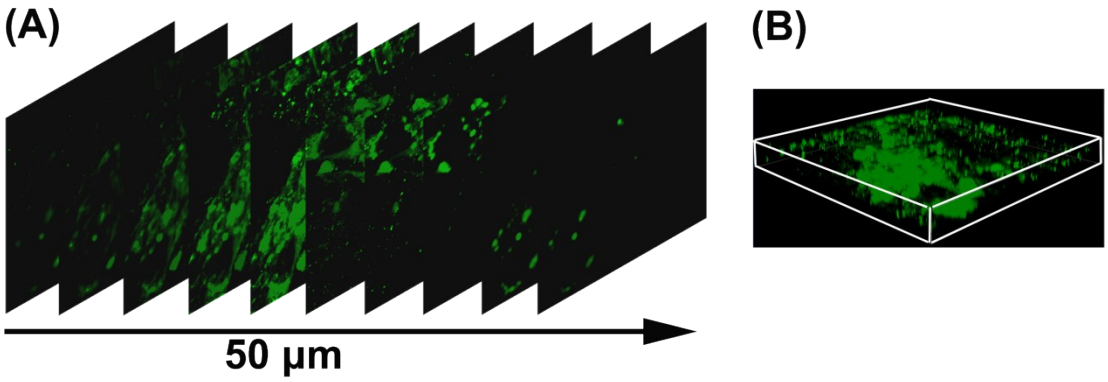

Fig. S18 Two-photon fluorescence images of the mormal heart slice pretreated with **MND-Lys** (15 μM). The images were collected at 500-550 nm with TP excitation of 800 nm.

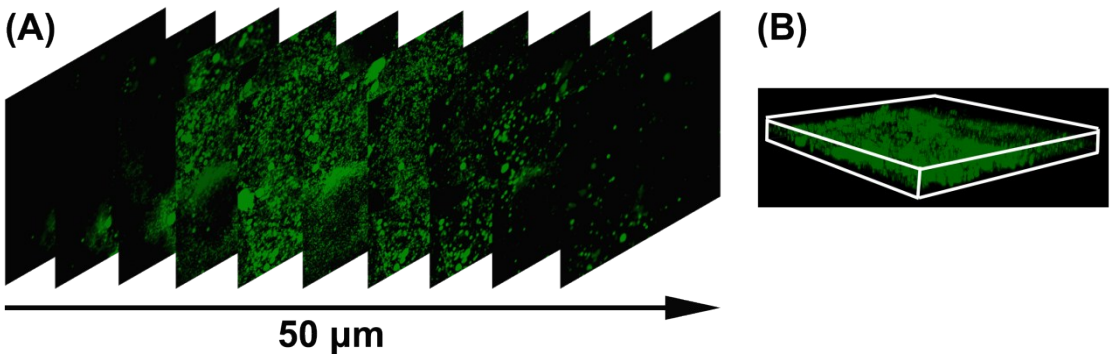

Fig. S19 Two-photon fluorescence images of the liver slice pretreated with **MND-Lys** (15 μM). The images were collected at 500-550 nm with TP excitation of 800 nm.

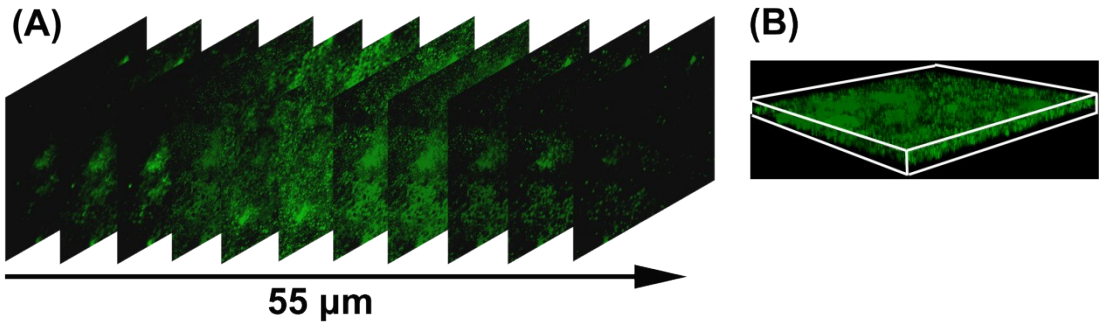

Fig. S20 Two-photon fluorescence images of the spleen slice pretreated with **MND-Lys** (15 μM). The images were collected at 500-550 nm with TP excitation of 800 nm.

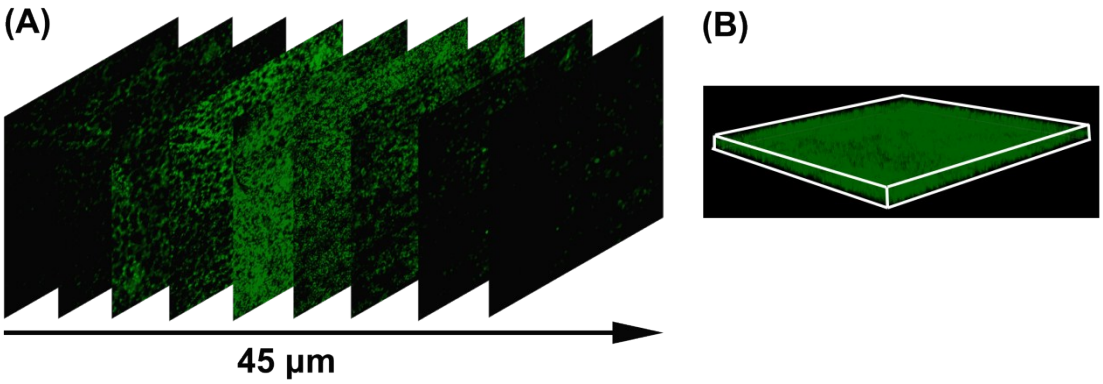

Fig. S21 Two-photon fluorescence images of the lung slice pretreated with **MND-Lys** (15 μM). The images were collected at 500-550 nm with TP excitation of 800 nm.

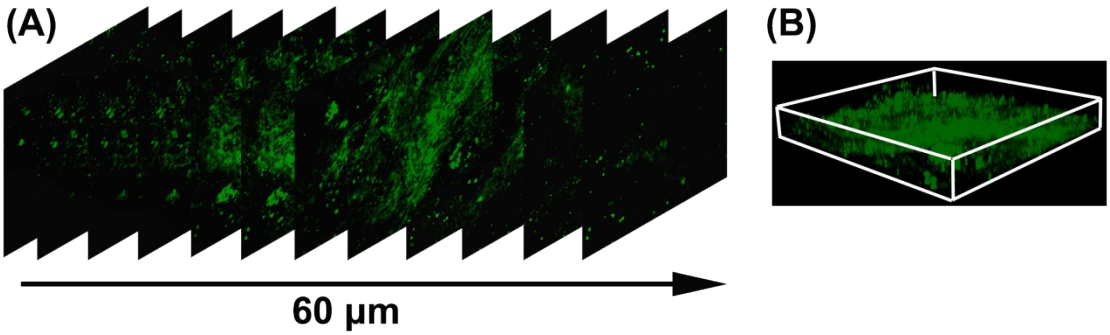

Fig. S22 Two-photon fluorescence images of the kidney slice pretreated with **MND-Lys** (15 μM). The images were collected at 500-550 nm with TP excitation of 800 nm.

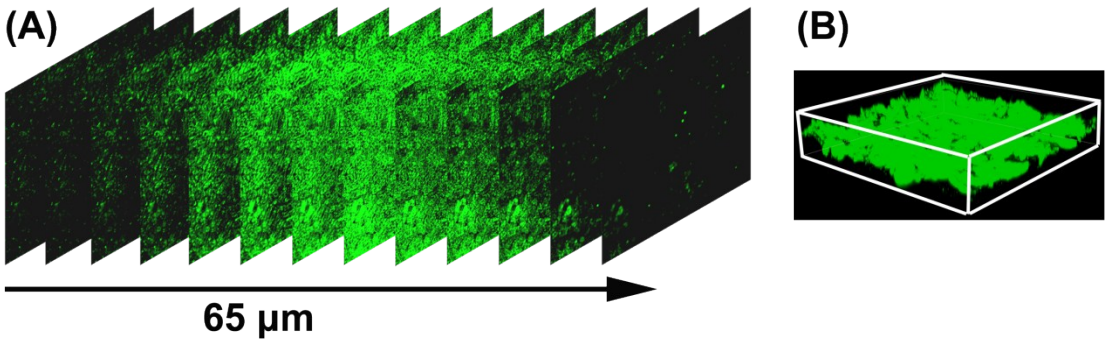

Fig. S23 Two-photon fluorescence images of the tumor slice pretreated with **MND-Lys** (15 μM). The images were collected at 500-550 nm with TP excitation of 800 nm.

Table S2. The weight (mg) of normal-feeding mice and high-fat feeding mice at different time points.

	0 Days	**5 Days**	**8 Days**	**12 Days**	**20 Days**
Normal Feeding	13915.9	14296.9	15050.3	15400.9	16015.7
High Fat Feeding	13915.8	15495.4	16773.6	17474.0	19869.8

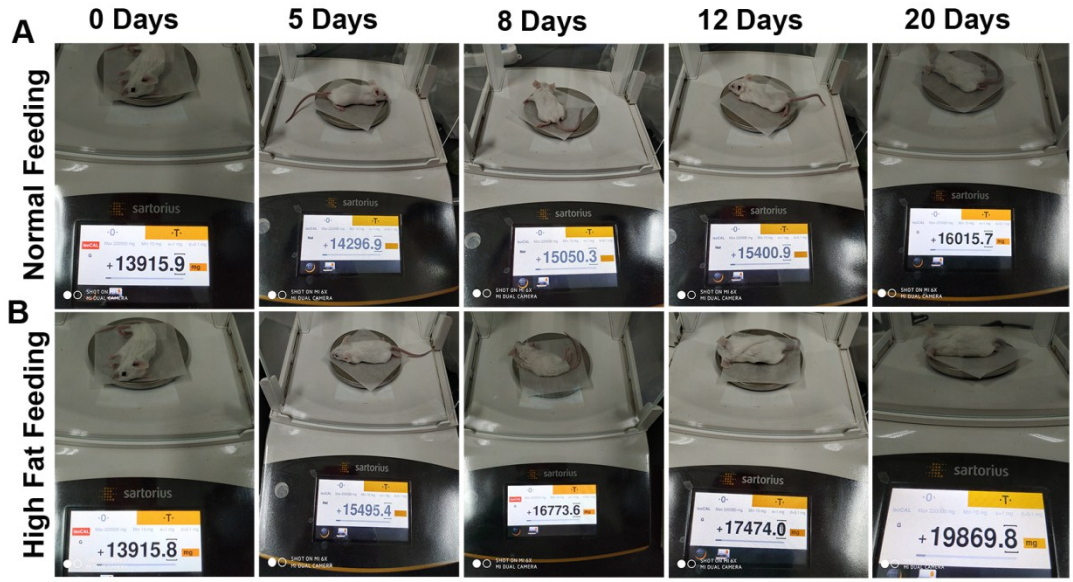

Fig. S24 The photos of weight (mg) changes at different time points normal-feeding mice (A) and high-fat feeding mice (B).

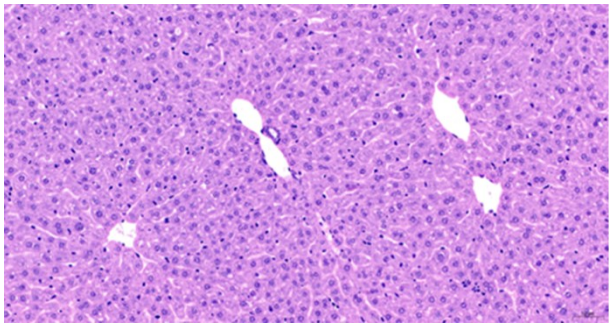

Fig. S25 Pathological changes of liver tissue in normal mice. The liver exhibits a uniform dark red color with sharp edges, which indicate no fatty liver disease.

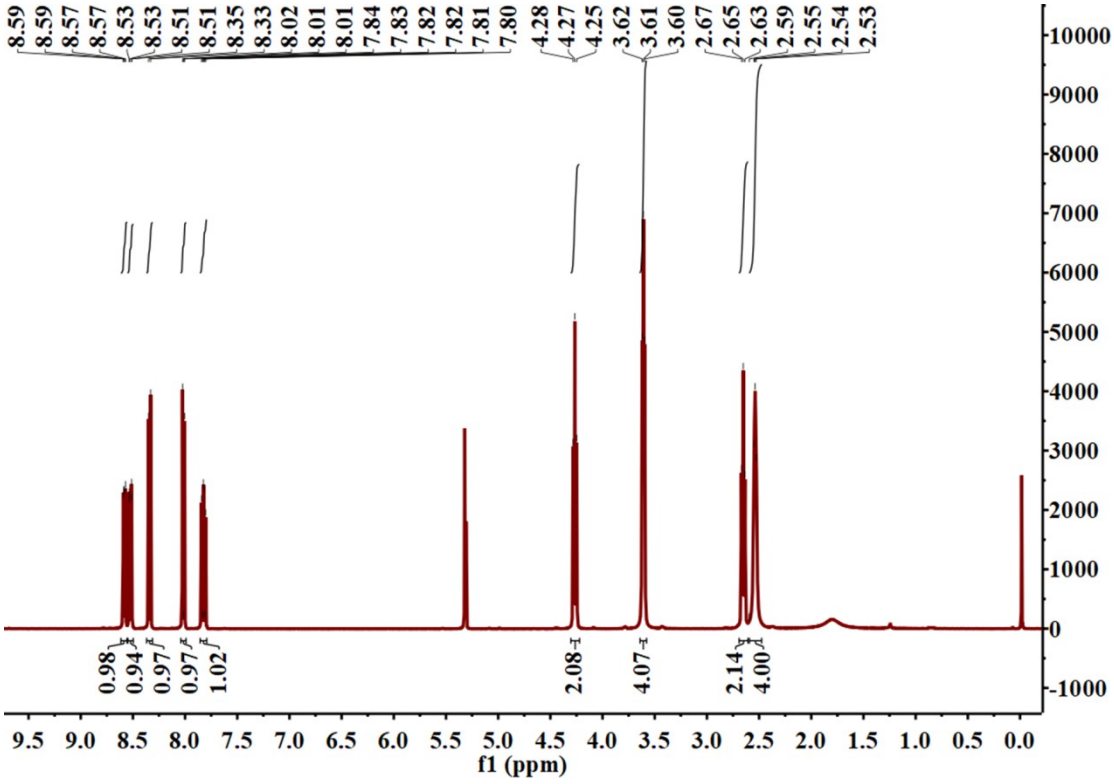

Fig. S26 The ^{1}H NMR spectrum of compound **1** in CD_2Cl_2.

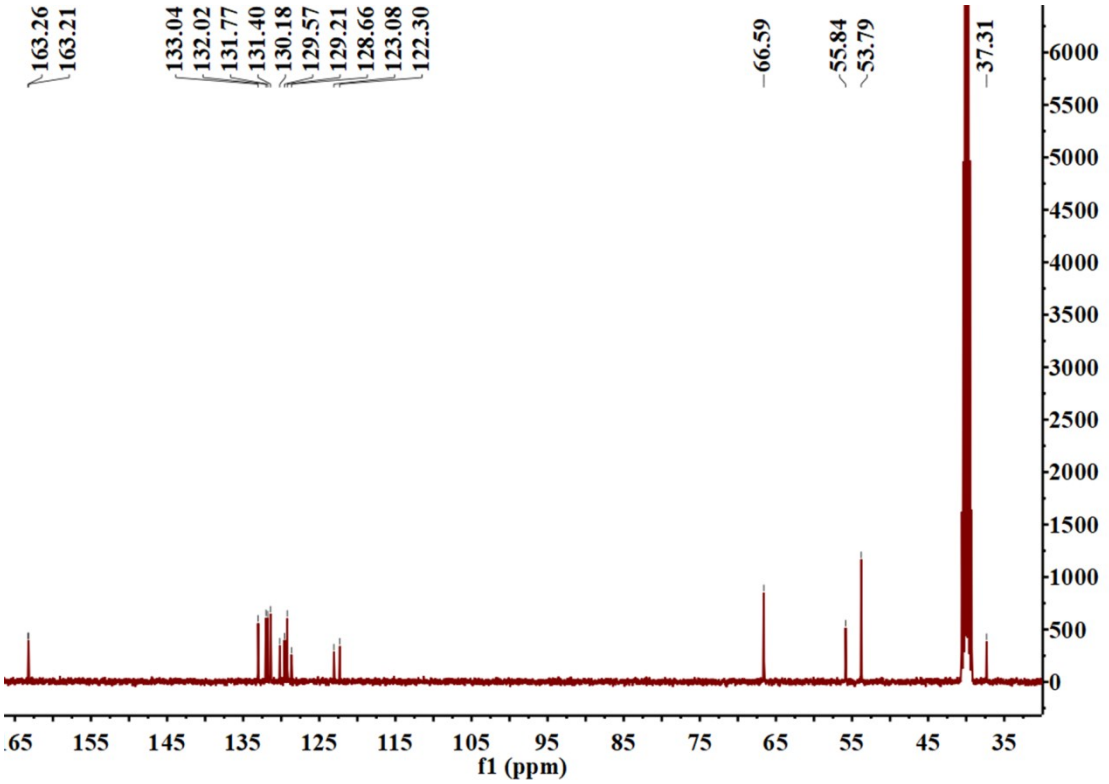

Fig. S27 The ^{13}C NMR spectrum of compound **1** in DMSO-*d6*.

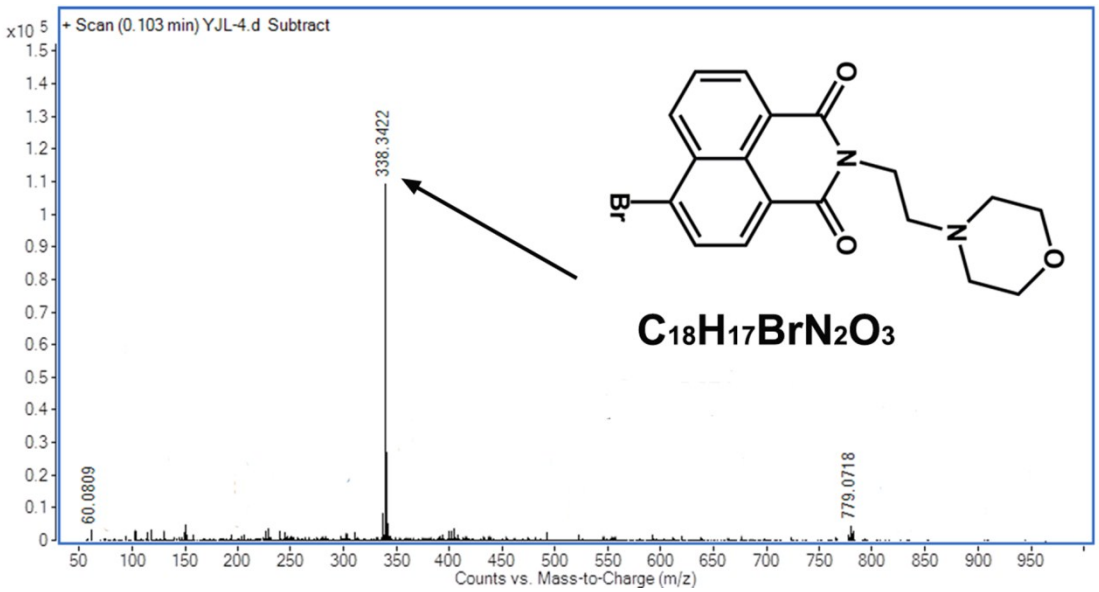

Fig. S28 The HRMS spectrum of compound **1**.

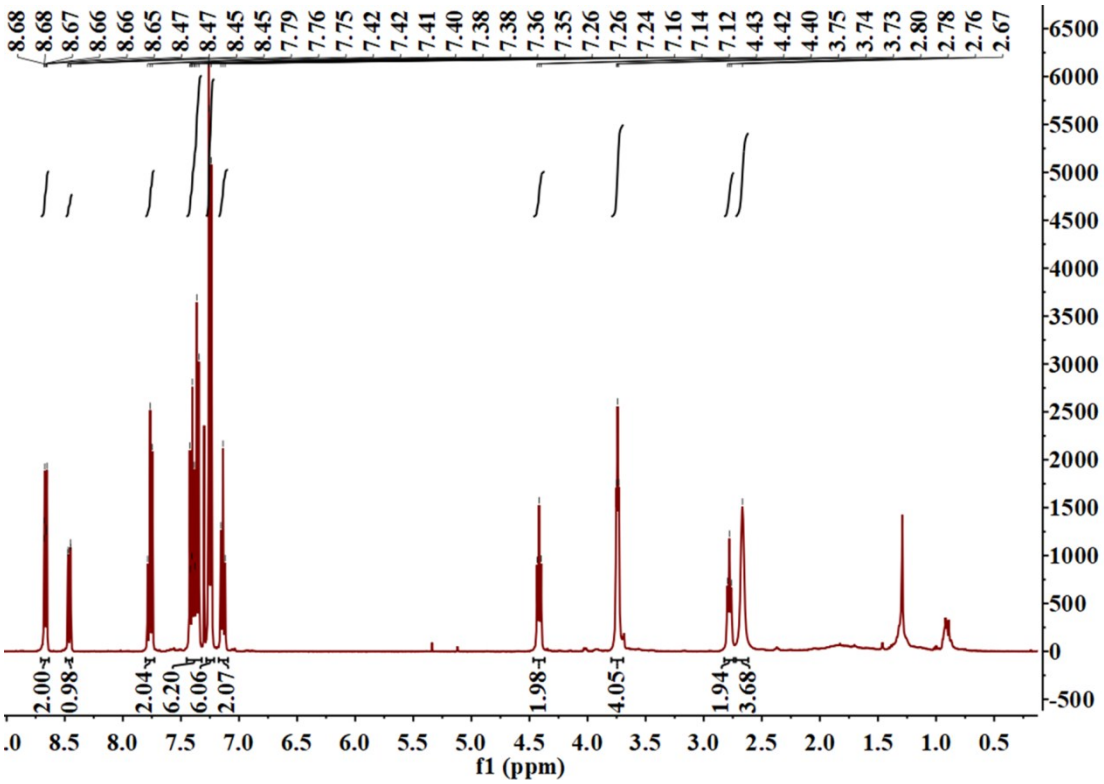

Fig. S29 The ^{1}H NMR spectrum of **MND-Lys** in chloroform-*d6*.

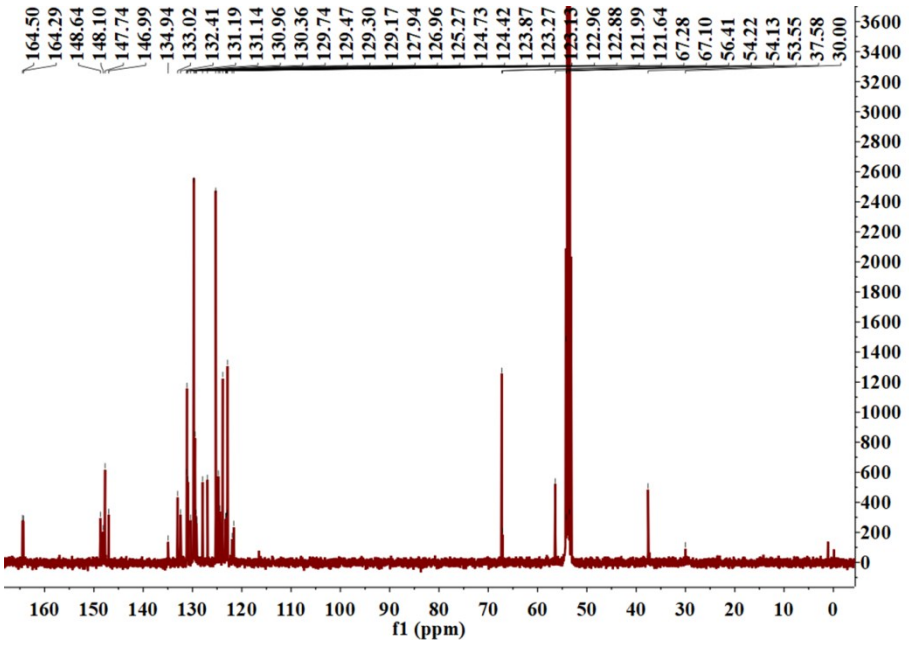

Fig. S30 The ^{13}C NMR spectrum of **MND-Lys** in CD_2Cl_2.

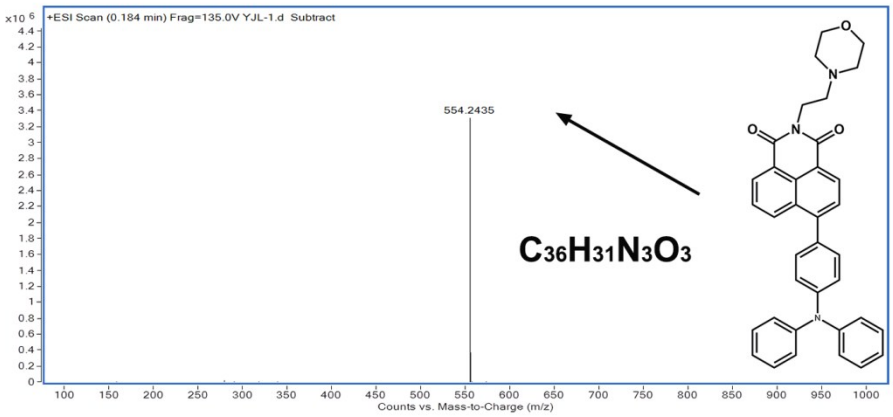

Fig. S31 The HRMS spectrum of **MND-Lys**.